

Takanori Sugimoto · Yasutoshi Sasaki

## Fatigue life of structural plywood under two-stage panel shear load: a new cumulative fatigue damage theory

Received: April 5, 2006 / Accepted: September 20, 2006 / Published online: March 11, 2007

**Abstract** The fatigue life of structural plywood under two-stage panel shear load was experimentally examined. Two experimental conditions were determined for two-stage fatigue of plywood specimen: one used variable applied stress and the other used variable stress, loading waveform, and loading frequency, because fatigue life of wood composite under constant load depended on loading waveform and loading frequency as well as stress level. The most famous cumulative fatigue damage theory is the Palmgren-Miner rule, which is the summation of the ratio of the applied loading cycle to the fatigue life under each loading stage. However, the applicability of this rule to the two-stage fatigue of wood composites has not been investigated. It was first demonstrated in this study that the fatigue life of the plywood specimen reached in the two-stage fatigue test did not obey the Palmgren-Miner rule. Here, we propose the new cumulative fatigue damage model by modification of the Palmgren-Miner rule on the basis of the assumption that fatigue damage accumulates with loading cycle on a logarithmic scale. The newly proposed model was in good agreement with the fatigue life reached in the two-stage fatigue test.

**Key words** Two-stage fatigue · Fatigue life · Palmgren-Miner rule · New cumulative fatigue damage model

### Introduction

Structural elements in timber structures are subjected to cyclic load in service, as in typhoons and earthquakes. When the service life becomes longer due to much attention to sustainable and environmentally friendly timber structures, wood and wood composites must bear a larger number of

cyclic loads. Therefore, there is a need to understand the fatigue properties of wood and wood composites in the structural design of timber construction for long-term performance.

Many studies have been conducted on the fatigue behavior of wood and wood composites under several mechanical conditions. For example, it was revealed that the number of loading cycles to failure, that is, fatigue life of solid wood in tension, compression, and torsion, was highly dependent on loading waveform and loading frequency as well as stress level.<sup>1–6</sup> Fatigue behavior of solid wood under combined axial and torsional load was also investigated.<sup>7–9</sup> In all of these studies, constant load under several mechanical conditions was repeatedly applied to the specimen throughout the fatigue test. Although actual load varies in peak value, waveform, and frequency during service, the fatigue behavior and damage development of wood and wood composites under variable load are not fully understood. Experimental studies on fatigue under variable load in peak stress, loading waveform, and loading frequency are necessary to evaluate the fatigue life under actual loading situations in the structural design.

The purpose of our research was to elucidate the fatigue behavior and damage mechanism of wood composite under variable load. Wood-based panels are frequently subjected to variable panel shear load in the case of the sheathing of shear walls and the web of complex beams. In this article, the fatigue life of structural plywood under two-stage panel shear load was experimentally examined, and the applicability of the Palmgren-Miner rule and a newly proposed cumulative fatigue damage model described in Theory was investigated.

### Theory

In the fatigue of load-bearing materials such as metal under variable load, the Palmgren-Miner rule<sup>10,11</sup> is the most famous of the cumulative fatigue damage theories. This rule has the following mathematical form:

T. Sugimoto · Y. Sasaki (✉)  
Graduate School of Bioagricultural Sciences, Nagoya University,  
Furo-cho, Chikusa-ku, Nagoya 464-8601, Japan  
Tel. +81-52-789-4148; Fax +81-52-789-4147  
e-mail: yasaki@nagoya-u.jp

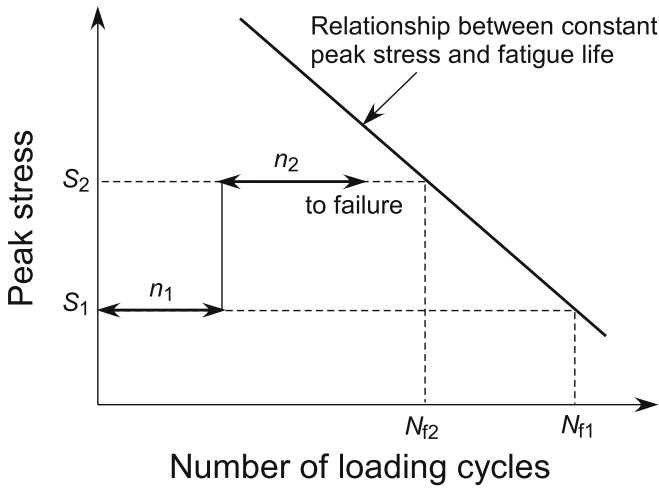


Fig. 1. Schematic illustration for two-stage fatigue

$$\Sigma(n_i/N_{fi}) = 1 \quad (1)$$

where  $n_i$  is the number of applied loading cycles at the  $i$ th loading stage, and  $N_{fi}$  is the fatigue life under constant stress at the  $i$ th loading stage. The measure of fatigue damage is simply the cycle ratio in this rule, that is,  $n_i/N_{fi}$  expresses the fatigue damage at the  $i$ th stage. Fatigue failure is considered to occur when  $\Sigma(n_i/N_{fi}) = 1$ . In two-stage fatigue as illustrated in Fig. 1, Eq. 1 is shown as follows:

$$n_1/N_{f1} + n_2/N_{f2} = 1 \quad (2)$$

It is well known that the fatigue of metal under variable load does not always follow the Palmgren-Miner rule, and many cumulative fatigue damage models have been developed. Unfortunately, none of them can achieve universal acceptance, and the Palmgren-Miner rule is still predominantly used in design.<sup>12</sup> In the fatigue of wood and wood composites, there has been no study on the applicability of this rule under variable load, although a few studies treated its application to fatigue in wood joints.<sup>13,14</sup>

In several studies on the fatigue of wood and wood composites,<sup>8,9,15-17</sup> the mechanical properties changed with the number of loading cycles on a logarithmic scale. This tendency was found to be common in different material configurations and loading modes such as tension, compression, and bending. We speculated from these results that fatigue damage of wood and wood composites might accumulate with increasing number of loading cycles on a logarithmic scale. Therefore, a new cumulative fatigue damage model for two-stage fatigue is proposed here by modification of the Palmgren-Miner rule as follows:

$$\log(n_1)/\log(N_{f1}) + [\log(n_1 + n_2) - \log(n_1)]/\log(N_{f2}) = 1 \quad (3)$$

We should note that the numerator of the second term is not  $\log(n_2)$ . When  $n_2$  is equal to 100 cycles, for example,  $n_2$  on a logarithmic scale is smaller at  $n_1 = 1000$  than at  $n_1 = 100$ . Accordingly, loading history should be taken into consideration on a logarithmic scale, as shown in Eq. 3. The new cumulative fatigue damage model can be extended to multistage fatigue as in the following equation:

Table 1. Specification of plywood panel

Specification	Comments
Grade	JAS structural plywood, type special, class 2
Laminated constitution	3 ply (2.30, 4.65, and 2.30 mm thickness)
Dimensions (mm)	1820 (L) × 910 (W) × 9 (T)
Wood species of veneer	Russian larch ( <i>Larix sibirica</i> Ledebour)
Adhesive	Alkali phenol resin adhesive

L, Panel length; W, panel width; T, panel thickness

$$\Sigma[\{\log[\Sigma(n_i)] - \log[\Sigma(n_{i-1})]\}/\log(N_{fi})] = 1 \quad (4)$$

where  $\log(n_0)$  is assumed to be zero. This model is phenomenological and as simple as the Palmgren-Miner rule.

## Materials and methods

### Specimens

Commercially available plywood was used in this study. Its specification is listed in Table 1. The density of plywood was  $0.55 \pm 0.02$  (g/cm<sup>3</sup>), and its moisture content was  $8.5\% \pm 0.4\%$  under the test conditions of 24°C (room temperature) and relative humidity of 55%.

Specimens were prepared from the plywood panel according to ASTM D 2719, "Method C; Two Rail Shear Test."<sup>18</sup> The peripheral edges were cut from each side of 9 plywood panels. Then 12 specimens of 350 mm (length) × 240 mm (width) were obtained from each panel. Width direction of the specimens was parallel to the fiber direction of the face veneer, as shown in Fig. 2a. Two specimens were extracted from each panel to obtain the static strength under panel shear load, while the others were used for the fatigue tests as shown in Fig. 2a. The size of the test specimens described above was smaller than the standard specimen size (610 × 406 mm) defined in ASTM D 2719 because the range of movement of the cross-yoke in our test machine was less than 600 mm.

To reinforce and hold the specimen for both static and fatigue tests under panel shear load, lumber splints with the density of 0.82 g/cm<sup>3</sup> were bonded to the longitudinal sides of each specimen with resorcinol resin glue. Bolt holes were bored to hold the specimen by two pairs of steel rails, as shown in Fig. 2b.

### Static test

In order to determine the static panel shear strength of test specimens, the static test was first performed prior to the fatigue test. Eighteen specimens were prepared for the static test, as mentioned above. From among these, 13 specimens were selected by visual inspection and actually used for the static test.

The static panel shear loading test was conducted according to ASTM D2719, Method C.<sup>18</sup> Two pairs of L-shaped steel rails were fastened to the specimen, as shown in Fig. 3. The upper rails were attached to the actuator of

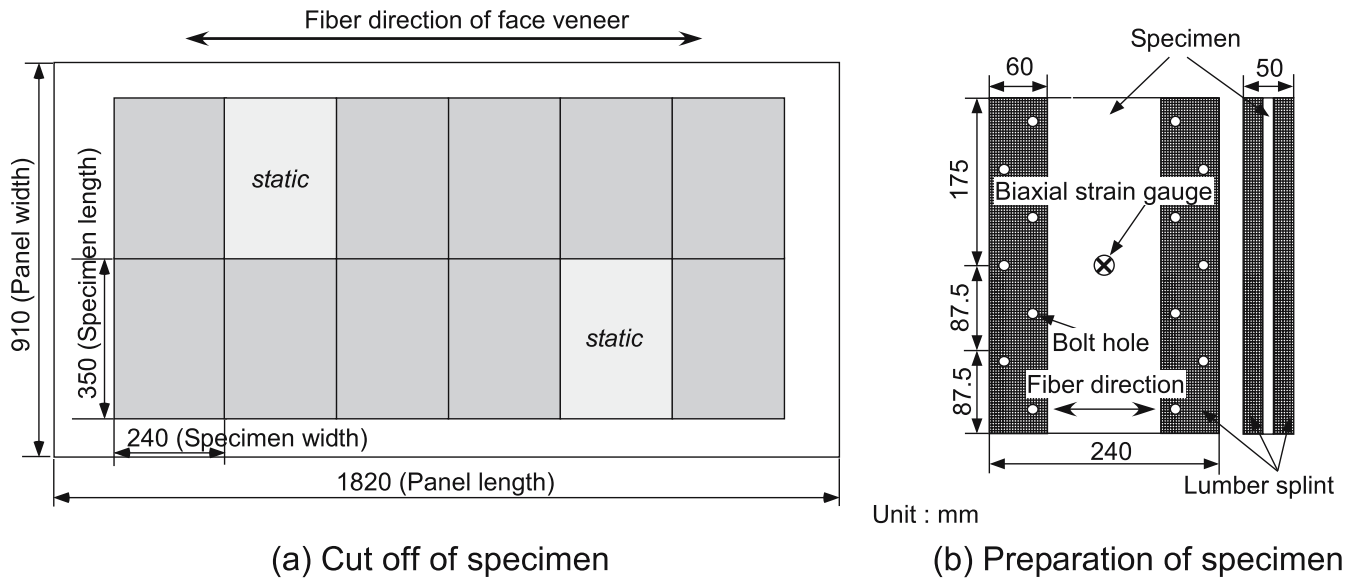


Fig. 2. Preparation of test specimen

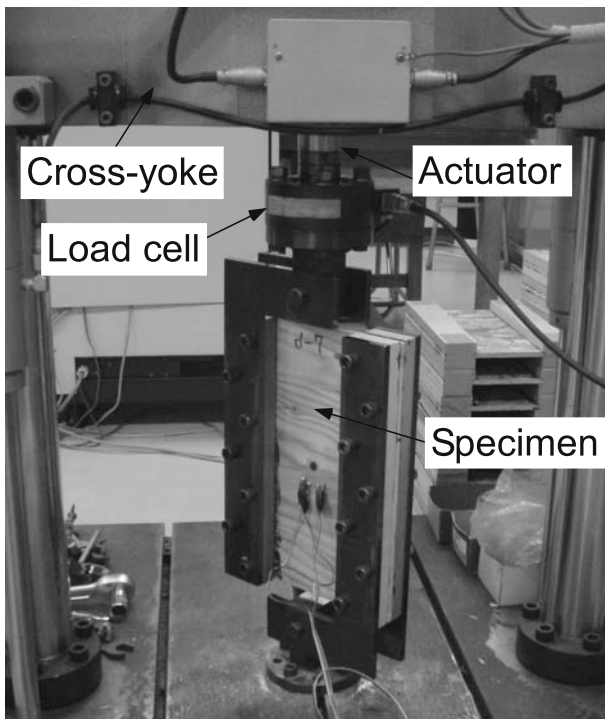


Fig. 3. Actual experimental setup for static and fatigue tests in panel shear load

an electrohydraulic servo fatigue testing machine (EHF-UB5-10L; Shimadzu, Kyoto, Japan), and the lower rails were fixed. Panel shear load was applied longitudinally to the specimen.

The static test was carried out under displacement control at a constant rate of 1.5 mm/min. Load and the displacement of the actuator were measured. Shear strain was also measured at the center of the specimen with a biaxial strain

Table 2. Static strength and rigidity in panel shear load

	$\tau_{\text{static}}$ (MPa)	$G$ (GPa)
Mean (nb = 13)	5.03	0.52
COV (%)	7.65	20.79

$\tau_{\text{static}}$ , Static panel shear strength;  $G$ , shear rigidity; nb, number of test specimens; COV, coefficient of variation

gauge (KFG-5-120-D16; Kyowa, Tokyo, Japan; 5 mm gauge length and 120  $\Omega$  resistance), as shown in Fig. 2b.

The results of the static test under panel shear load are listed in Table 2. Static strength of each specimen ( $\tau_{\text{max}}$ ) was calculated using:

$$\tau_{\text{max}} = P_{\text{max}}/(lt) \quad (5)$$

where  $P_{\text{max}}$  is the maximum applied load, and  $l$  and  $t$  are the length and the thickness of each specimen, respectively. The mean value of static strength obtained from the 13 specimens ( $\tau_{\text{static}}$ ) was used as the reference standard of applied stress in the fatigue test.

Shear rigidity ( $G$ ) was evaluated using

$$G = \Delta\tau/\Delta\gamma \quad (6)$$

where  $\Delta\tau$  is the increment of shear stress, and  $\Delta\gamma$  is the increment of shear strain. In the case of the static test,  $\Delta\tau$  was determined to be in the range of 10%–30% of static strength.

### Fatigue test

The fatigue test of plywood specimen was designed to perform in the experimental conditions as listed in Tables 3–5. In the two-stage fatigue test of metals, the value of applied stress level is generally determined for the experimental condition. Fatigue life of wood and wood composites depends on not only the stress level but also on loading condi-

tions such as loading waveform and frequency, as described in the Introduction. That is to say, both applied stress and loading conditions probably influence the fatigue damage of wood and wood composites. Variable load in peak stress value, loading waveform, and frequency is applied to wood and wood composites during service. Therefore, two experimental conditions were determined for two-stage fatigue of plywood specimens: one case in variable applied stress and another in variable stress, loading waveform, and loading frequency.

For the first experimental condition (referred to as “one-stage fatigue”), the fatigue test was conducted in three loading conditions determined by loading waveform and frequency to obtain the relationship between constant peak stress ( $S$ ) and fatigue life ( $N_f$ ) in different loading conditions. Loading waveform was selected to be square or triangular in a nonreversible fashion, and frequency was set as 0.5 or 5.0 Hz, as listed in Table 3. Applied peak stresses

**Table 3.** Experimental conditions in one-stage fatigue

Loading waveform	Loading frequency (Hz)	Peak stress $S$ (MPa)
Square (Sq)	0.5	4.64
	0.5	3.61
	0.5	2.58
Triangular (Tr)	0.5	4.64
	0.5	3.61
	0.5	2.58
Triangular (Tr)	5.0	4.64
	5.0	3.61
	5.0	2.58

had three set points in each loading condition. Peak stress, loading waveform, and frequency were fixed throughout the test of each specimen. For the second experimental condition (referred to as “two-stage fatigue I”), peak stress was changed once during the test of each specimen, and loading waveform and frequency were fixed as the triangular waveform and 0.5 Hz. Four patterns for changing the peak stress were established in the High–Low and Low–High loading groups, respectively, as listed in Table 4. The number of loading cycles for the first stage ( $n_1$ ) was preset in each pattern, and the number of loading cycles for the second stage ( $n_2$ ) was experimentally obtained by the fatigue failure of each specimen. Not only peak stress but also loading waveform and frequency were simultaneously changed at respective loading cycles in the third experimental condition (referred to as “two-stage fatigue II”). Two different changing patterns were established in each High–Low and Low–High loading group, as listed in Table 5. Specimens obtained from five plywood panels were prepared for one-stage fatigue, and those from four other panels were for two-stage fatigue I and II. Three specimens were used for each loading pattern. That is, 27 specimens were tested in one-stage fatigue, 24 specimens in two-stage fatigue I, and 12 specimens in two-stage fatigue II.

The fatigue test under panel shear load was conducted with the same experimental setup as that used for the static test. Load, the displacement of the actuator, and shear strain were recorded simultaneously with a dynamic data logger (PCD-1000; Kyowa). During the fatigue test, the strain gauge failed at a large number of loading cycles, after which shear strain was compared with the total deformation

**Table 4.** Experimental conditions in two-stage fatigue I

	First stage		Second stage	
	$S_1$ (MPa)	$n_1$ (cycle)	$S_2$ (MPa)	$n_2$ (cycle)
High–Low loading				
HL1	3.86	500	3.38	
HL2	4.34	50	2.89	
HL3	4.34	1	3.38	
HL4	4.34	10	3.86	
To failure				
Low–High loading				
LH1	2.89	50000	4.34	
LH2	3.38	5000	3.86	
LH3	3.38	5	4.34	
LH4	3.86	10	4.34	

$S_i$ , Peak stress at  $i$ th stage;  $n_i$ , number of loading cycles at  $i$ th stage ( $i = 1, 2$ )

**Table 5.** Experimental conditions in two-stage fatigue II

	First stage				Second stage			
	Waveform	Frequency (Hz)	$S_1$ (MPa)	$n_1$ (cycle)	Waveform	Frequency (Hz)	$S_2$ (MPa)	$n_2$ (cycle)
High–Low loading								
HLa	Sq	0.5	3.86	30	Tr	0.5	3.38	
HLb	Tr	0.5	4.34	3	Tr	5.0	3.38	
To failure								
Low–High loading								
LHa	Tr	0.5	3.38	10	Sq	0.5	3.86	
LHb	Tr	5.0	3.38	10000	Tr	0.5	4.34	

$S_i$ , Peak stress at  $i$ th stage;  $n_i$ , number of loading cycles at  $i$ th stage ( $i = 1, 2$ ); Sq, square; Tr, triangular

of the specimen calculated from the displacement of the actuator.<sup>17</sup> All the tests were carried out at a room temperature of 24°C and relative humidity of 55%. The mechanical analyses based on these measurements were not included in this article, and those detailed results will be reported in the following articles.

**Results and discussion**

Relationship between peak stress and fatigue life in one-stage fatigue

As shown in Fig. 4, the fatigue life of the plywood specimen obtained in one-stage fatigue was longer at lower stress level, and was highly dependent on loading waveform and frequency, as described in other studies on the fatigue of solid wood described in the Introduction. Fatigue life of plywood specimens for a set peak stress was longer in the order of the square waveform at the loading frequency of 0.5 Hz, triangular waveform at 0.5 Hz, and triangular waveform at 5.0 Hz. It was roughly estimated from these results that the fatigue damage caused by one loading cycle was probably smaller in the same order. There exist negative linear relationships between peak stress and fatigue life on a logarithmic scale for each loading condition. Every regression line was statistically significant at the 1% significance level. These regression lines are standards for the calculation based on cumulative fatigue damage theory, as described below.

Fatigue life in two-stage fatigue I and II

Fatigue life of plywood specimens obtained in two-stage fatigue I and II were plotted against the peak stress at the first stage ( $S_1$ ), as shown in Fig. 5. Fatigue life in two-stage

fatigue is the sum of the number of loading cycles at the first stage ( $n_1$ ) and that at the second stage ( $n_2$ ). In two-stage fatigue I, the plots for High–Low loading groups (HL1–HL4) were positioned at the right of the regression line obtained in one-stage fatigue, and those for Low–High loading groups (LH1–LH4) were at the left of the line. The specimens of High–Low loading groups were subjected to lower peak stress at the second stage ( $S_2$ ) than that at the first stage ( $S_1$ ). Then their fatigue lives were longer than those for one-stage fatigue under constant peak stress equal to  $S_1$ . On the other hand, the fatigue life of Low–High loading groups resulted in shorter fatigue lives than those for one-stage fatigue.

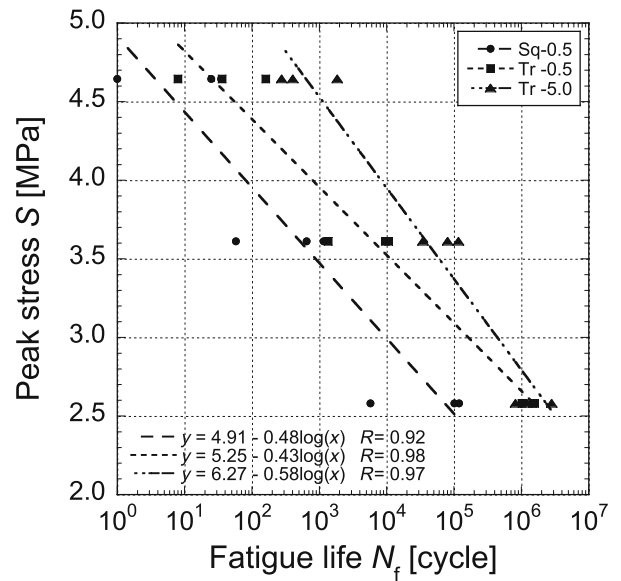


**Fig. 4.** Relationships between peak stress ( $S$ ) and fatigue life ( $N_f$ ) obtained in one-stage fatigue

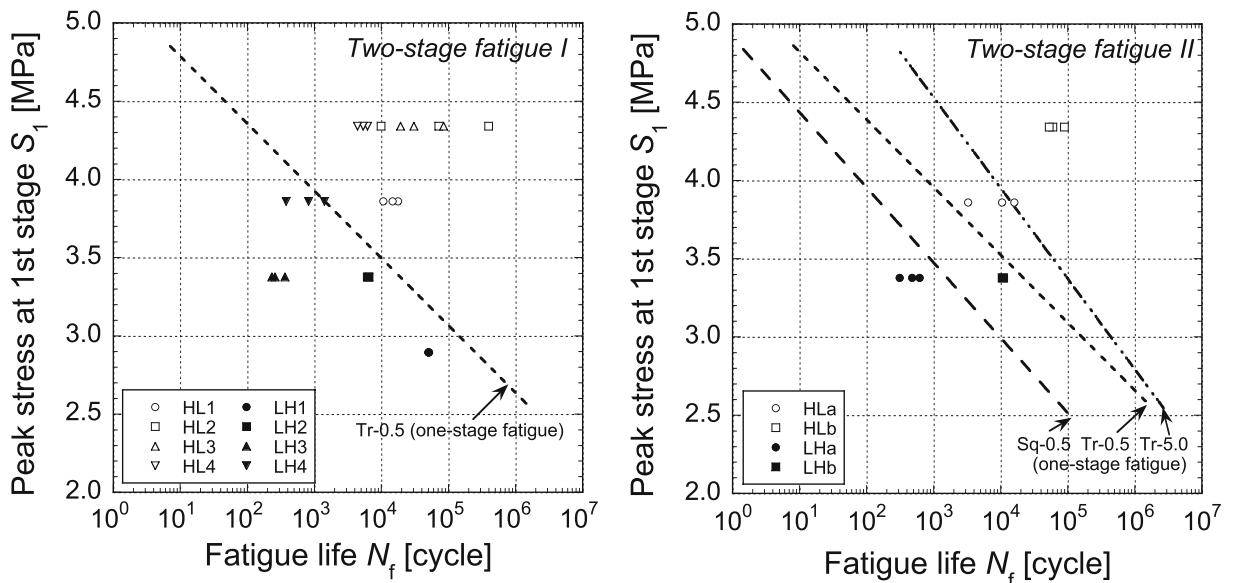


**Fig. 5.** Fatigue life obtained in two-stage fatigue I (left) and II (right)



Similar tendency for High–Low and Low–High loading was also observed in two-stage fatigue II. For example, when the waveform was changed from square to triangular, and the peak stress was from 3.86 ( $S_1$ ) to 3.38MPa ( $S_2$ ) in the “HLa” condition, the fatigue damage was estimated to be smaller for the triangular waveform than for the square waveform, as described above, and also smaller at lower peak stress. Then the fatigue lives in the HLa condition were longer than those at  $S_1$  for one-stage fatigue with square waveform and frequency of 0.5Hz and shorter than those at  $S_2$  for one-stage fatigue with triangular waveform and the same frequency.

#### Applicability of cumulative fatigue damage theories

The mathematical form of the Palmgren-Miner rule in two-stage fatigue is described as Eq. 2. The first and second term of Eq. 2 were plotted in Fig. 6 along the  $x$  and  $y$  axes, respectively, for all specimens tested in two-stage fatigue I and II. Fatigue life at constant peak stress equal to  $S_1$  ( $N_{f1}$ ) and that at constant peak stress equal to  $S_2$  ( $N_{f2}$ ) were calculated with the regression lines obtained in one-stage fatigue shown in Fig. 4. In two-stage fatigue I, loading waveform and frequency were fixed as the triangular waveform and 0.5Hz, and the peak stress was changed during the fatigue test. Then,  $N_{f1}$  and  $N_{f2}$  were calculated with the regression line for the triangular waveform and frequency of 0.5Hz according to respective peak stress. Loading waveform and frequency as well as peak stress were simultaneously changed in two-stage fatigue II. In that case,  $N_{f1}$  and  $N_{f2}$  were calculated with a different regression line according to respective loading waveform, frequency, and peak stress. If the two-stage fatigue I and II of a plywood specimen is explained by the Palmgren-Miner rule, the experimental plots lie on the theoretical straight line that connects unity on the  $x$  and  $y$  axes. However, the plots scattered significantly away from the straight line. These results demonstrated for the first time that the Palmgren-Miner rule could not account for the two-stage fatigue of a plywood specimen under panel shear load.

Then the new cumulative fatigue damage model proposed in Theory was applied to the results obtained in both two-stage fatigue I and II. The first and second terms of Eq. 3 were plotted along the  $x$  and  $y$  axes, respectively, in Fig. 7. All experimental plots were found to lie almost on the theoretical straight line expressing the new cumulative fatigue damage model, although there was some scatter. Experimental plots apparently agree better with the theoretical line for the new cumulative fatigue damage model than the line for the Palmgren-Miner rule, as shown by comparison of Figs. 6 and 7. Therefore, these results indicate that the new cumulative fatigue damage model could be applicable to the two-stage fatigue of a plywood specimen under variable panel shear load in peak stress, loading waveform, and loading frequency. This is the great advantage of the new cumulative fatigue damage model, because the applied stress value and loading condition definitely influence the fatigue life of wood composite.

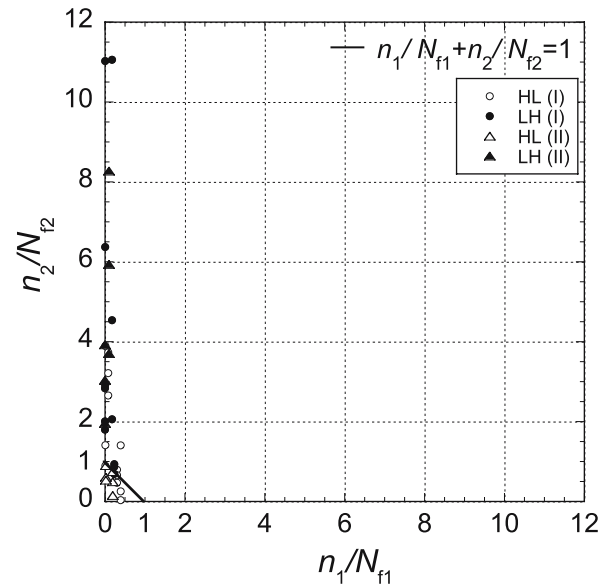


Fig. 6. Application of the Palmgren-Miner rule to two-stage fatigue I and II. HL, High–Low loading group; LH, Low–High loading group

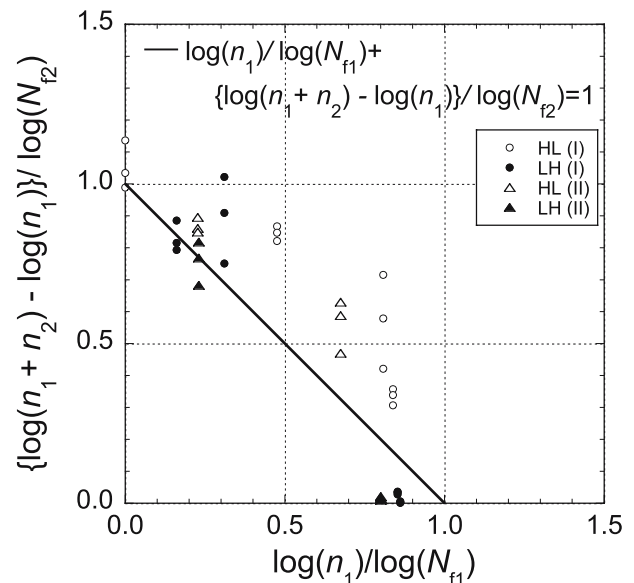


Fig. 7. Application of the new cumulative fatigue damage model to two-stage fatigue I and II

## Conclusions

Fatigue testing of structural plywood under two-stage panel shear load was conducted with variation in peak stress, loading waveform, and loading frequency. Applicability of the Palmgren-Miner rule and the newly proposed cumulative fatigue damage model was investigated. This article is the first report to state that the fatigue life of a plywood specimen in two-stage fatigue did not obey the Palmgren-Miner rule. The newly proposed cumulative fatigue damage model can definitely be applied to the two-stage fatigue of plywood specimens.

In the articles that will follow this report, fatigue-induced changes in the mechanical properties and the damage mechanism of plywood specimens under two-stage fatigue load will be reported in detail.

---

## References

- Okuyama T, Itoh A, Marsoem SN (1984) Mechanical responses of wood to repeated loading I. Tensile and compressive fatigue fractures. *Mokuzai Gakkaishi* 30:791–798
- Marsoem SN, Bordonné PA, Okuyama T (1987) Mechanical responses of wood to repeated loading II. Effect of wave form on tensile fatigue. *Mokuzai Gakkaishi* 33:354–360
- Kohara M, Okuyama T (1994) Mechanical responses of wood to repeated loading VII. Dependence of energy loss on stress amplitude and effect of wave forms on fatigue lifetime. *Mokuzai Gakkaishi* 40:491–496
- Clorius CO, Pederson MU, Hoffmeyer P, Damkilde L (2000) Compressive fatigue in wood. *Wood Sci Technol* 34:21–37
- Gong M, Smith I (2003) Effect of waveform and loading sequence on low-cycle compressive fatigue life of spruce. *J Mater Civil Eng* 15:93–99
- Ando K, Yamasaki M, Watanabe J, Sasaki Y (2005) Torsional fatigue properties of wood (in Japanese). *Mokuzai Gakkaishi* 51:98–103
- Sasaki Y, Yamasaki M (2002) Fatigue strength of wood under pulsating tension-torsion combined loading. *Wood Fiber Sci* 34:508–515
- Sasaki Y, Yamasaki M (2004) Effect of pulsating tension-torsion combined loading on fatigue behavior in wood. *Holzforschung* 58:666–672
- Sasaki Y, Yamasaki M, Sugimoto T (2005) Fatigue damage in wood under pulsating multiaxial-combined loading. *Wood Fiber Sci* 37:232–241
- Palmgren A (1924) Die Lebensdauer von Kugellagern. *Verfahrenstechnik* 68:339–341
- Miner MA (1945) Cumulative damage in fatigue. *J Appl Mech* 67: A159–A164
- Fatemi A, Yang L (1998) Cumulative fatigue damage and life prediction theories: a survey of the state of the art for homogeneous materials. *Int J Fatigue* 20:9–34
- Hayashi T, Sasaki H (1984) Fatigue damage of wood butt-joints with metal-plate connectors (in Japanese). *Mokuzai Gakkaishi* 30:23–31
- Zhang J, Quin F, Tackett B (2001) Bending fatigue life of two-pin dowel joints constructed of wood and wood composites. *Forest Prod J* 51:73–78
- Thompson RJH, Bonfield PW, Dinwoodie JM, Ansell MP (1996) Fatigue and creep in chipboard. Part 3. The effect of frequency. *Wood Sci Technol* 30:293–305
- Hacker CL, Ansell MP (2001) Fatigue damage and hysteresis in wood-epoxy laminates. *J Mater Sci* 36:609–621
- Sugimoto T, Yamasaki M, Sasaki Y (2006) Fatigue and hysteresis effects in wood-based panels under cyclic shear load through thickness. *Wood Fiber Sci* 38:215–228
- American Society for Testing and Materials (ASTM) (2005) ASTM D2719. Standard test method for structural panels in shear through-the-thickness, vol 04.10. Wood. Section-7. American Society for Testing and Materials, West Conshohocken, PA, pp 395–403